Computers and Concrete, Vol. 8, No. 5 (2011) 597-616
DOI: http://dx.doi.org/10.12989/cac.2011.8.5.597

Modeling the confined compressive strength of hybrid circular concrete columns using neural networks

Andres W.C. Oreta* and Jason M.C. Ongpeng

De La Salle University 2401 Taft Ave., Manila, Philippines

(Received June 23, 2009, Revised March 16, 2010, Accepted March 16, 2011)

Abstract. With respect to rehabilitation, strengthening and retrofitting of existing and deteriorated columns in buildings and bridges, CFRP sheets have been found effective in enhancing the performance of existing RC columns by wrapping and bonding CFRP sheets externally around the concrete. Concrete columns and piers that are confined by both lateral steel reinforcement and CFRP are sometimes referred to as "hybrid" concrete columns. With the availability of experimental data on concrete columns confined by steel reinforcement and/or CFRP, the study presents modeling using artificial neural networks (ANNs) to predict the compressive strength of hybrid circular RC columns. The prediction of the ultimate confined compressive strength of RC columns is very important especially when this value is used in estimating the capacity of structures. The present ANN model used as parameters for the confining materials the lateral steel ratio (ρ_s) and the FRP volumetric ratio (ρ_{FRP}). The model gave good predictions for three types of confined columns: (a) columns confined with steel reinforcement only, (b) CFRP confined columns, and (c) hybrid columns confined by both steel and CFRP. The model may be used for predicting the compressive strength of existing circular RC columns confined with steel only that will be strengthened or retrofitted using CFRP.

Keywords: confined concrete; column; compressive strength; carbon fiber; neural network; retrofit.

1. Introduction

Confined concrete may be described as concrete which when subjected to uni-axial compression is prevented from lateral "swelling". Confinement in concrete is effective only from the instant that internal cracking causes an increase in volume resulting into what is termed as passive confinement. Passive confinement results in the enhancement of the compressive strength of concrete and increase of ductility. The most common method of providing confinement in circular concrete columns is by installing transverse steel reinforcement in the form of closed ties, hoops or spirals around the perimeter of the longitudinal steel. Recently, new materials using fiber-reinforced polymer (FRP) have started to be used as confining devices in new columns - replacing the conventional steel reinforcement ties and spirals. With respect to rehabilitation, strengthening and retrofitting of existing and deteriorated columns in buildings and bridges, FRP sheets have now become very popular devices in enhancing the performance of existing RC columns by wrapping and bonding FRP sheets externally around the concrete. There are different types of FRP depending on the fiber material used – aramid, glass and carbon. These FRP sheets are installed by wrapping the concrete column externally using epoxy as an adhesive. Among the different types of FRP, carbon fiber-reinforced

* Corresponding author, Professor, E-mail: andyoreta@yahoo.com

polymer (CFRP) is found to have ideal characteristics as an external reinforcement and seems to be a popular fiber material. Concrete columns and piers that are confined by both lateral steel reinforcement and FRP are sometimes referred to as "hybrid" concrete columns.

The enhancement of the compressive strength of concrete columns due to confinement is reflected by an increase of the peak stress of the unconfined compressive strength (f'_{co}) to the confined compressive strength (f'_{cc}). Models for steel-confined columns using analytical or empirical equations (Mander *et al.* 1998a, Saatcioglu and Razvi 1992, Hoshikuma *et al.* 1997) have been developed to predict the confined compressive strength. Early investigations attempted to extend the steel-based models of Mander *et al.* (1998a) to FRP-confined columns such as Saadatmanesh *et al.* (1994) but the application was found inaccurate and often conservative. Hence, empirical models specifically suited to FRP-confined concrete columns or cylinders were proposed. De Lorenzis and Tepfers (2003) in his review of confinement models using FRP concluded that the three most accurate models are those by Samaan *et al.* (1998), Saafi *et al.* (1997) and Spoelstra and Monti (1999). Li *et al.* (2003) also proposed a confinement model for FRP-confined columns based on the mechanism of soil under tri-axial loading and used the Mohr-Columb failure envelope for soil.

Existing reinforced concrete columns when retrofitted by wrapping FRP sheets around the cylinder will be confined in the inner core by the lateral steel reinforcement and externally by the FRP sheets. The total lateral pressure exerted by the concrete core due to dilation of the column will be resisted by the two confining materials. Models for hybrid columns (e.g. Hosotani and Kawashima 1999, Li and Fang 2004) assumed that the confining pressure due to the two materials can be obtained by a simple superposition of the steel-based and FRP-based models. When these two materials are used together as confinement in a hybrid column - CFRP bonded externally around the column and steel wrapped around the longitudinal steel - the different properties of steel and CFRP may develop a complex interrelationship between the two confining materials and this may affect the compressive strength and over-all performance of the concrete column.

Most of the empirical and analytical equations for predicting the confined compressive strength of RC columns were developed using regression analysis of experimental data. Empirical models using regression analysis are developed by first assuming the form of the empirical equation and then the coefficients are obtained by fitting the data. The main problem with of this approach is that it is difficult to determine the form and the number of coefficients of the equation which will best describe the physical process. With this approach, different expressions have been derived – ranging from simple to complex, linear to nonlinear – depending on the assumptions and details of the experimental data used by the researchers. Because of the restriction of the assumed form of the equation, the model may not be able to capture the interrelationship of the various parameters considered in the model. Recently, researchers have found the potential of artificial neural networks (ANNs) in the modeling of various engineering and natural systems. ANNs have been found very powerful in modeling systems governed by multiple variable interrelationships, especially when the data available are "noisy" or incomplete. One advantage of neural network modeling is that there is no need to know a priori the functional relationship among the various variables involved, unlike in regression analysis. The ANNs automatically construct the relationships for a given network architecture as experimental data are processed through a learning algorithm. This approach is "data driven", meaning that the network adopts to the training data presented to capture the relationship among input and output parameters. Recognizing the potential of ANNs in modeling, there were a few attempts where ANNs were applied to strength prediction of RC columns. Chuang *et al.* (1998) demonstrated the feasibility of using multilayer feed forward neural networks to predict the

ultimate capacity of pin-ended slender RC columns under static loading. Oreta and Kawashima (2003), on the other hand, demonstrated the application of neural networks in predicting the confined compressive strength and strain of circular concrete columns confined with lateral steel ties and in simulating the effect of varying parameters such as the lateral and longitudinal steel ratios on the peak strength and strain. Cevik and Guzelbey (2008) derived an empirical equation using neural networks for predicting the strength enhancement of CFRP confined cylinders in terms of diameter, unconfined concrete strength, tensile strength of CFRP and total thickness of CFRP layer.

With more experimental data on concrete columns confined by steel reinforcement and/or CFRP becoming available, this study presents a neural network model specifically designed for predicting the compressive strength of hybrid concrete columns and also applicable to columns confined by steel reinforcement or CFRP only. A neural network model for predicting the compressive strength of circular concrete columns confined with steel reinforcement and/or CFRP may be a useful tool in the strengthening and retrofitting of existing structures.

2. Models for confined concrete columns

The effectiveness of confinement is reflected by an increase of the compressive strength of the concrete column over its unconfined value (f'_{co}). The confined compressive strength of concrete (f'_{cc}) is an enhanced strength due to confinement. When the axial compressive stress increases resulting to lateral expansion of the column, the confining devices develop a tensile hoop stress, which is balanced by a uniform radial confining pressure (p). Confined concrete is subjected to a state of tri-axial stress. The expressions for the confining pressure (p) have been derived using triaxial models similar to hydrostatic pressure or Mohr-Columb failure envelope for soil. In these models, the confined compressive strength of concrete (f'_{cc}) is generally assumed to be related to the confinement pressure (p) due to the steel reinforcement or FRP sheet. A simple expression for the confined strength of concrete is given as

$$f'_{cc} = f'_{co} + k_1 p \tag{1}$$

The expressions for confinement pressure (p) depends on the confining device (steel reinforcement or FRP). This uniform pressure can be derived from an equilibrium of forces as shown in Fig. 1. The confinement effectiveness coefficient (k_l) depends on the assumptions of the researchers and experimental data used.

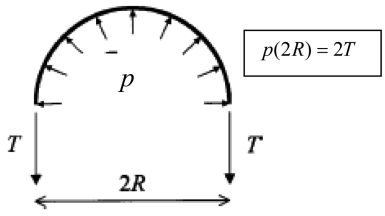

Fig. 1 Equilibrium of confined concrete

Table 1 Steel-based confinement models

Reference	Model
Mander *et al.* (1998)	$f'_{cc} = f'_{co}(2.254\sqrt{1+7.94k_e p_s/f'_{co}} - 2k_e p_s/f'_{co} - 1.254)$ where $k_e = (1-s/2d)^n/(1-\rho_{cc})$, $n=1$ for circular spirals and $n=2$ for circular hoops
Saatcioglu and Razvi (1992)	$f'_{cc} = f'_{co} + 6.7(\rho_s f_{ys}/2)^{0.83}$
Hoshikuma *et al.* (1997)	$f'_{cc} = f'_{co} + 3.83\rho_s f_{ys}$

2.1 Steel-confined concrete columns

The confined compressive strength of concrete with lateral steel can be expressed as the sum of the unconfined compressive strength (f'_{co}) and the increase in strength due to steel confinement (f'_{cs}) as $f'_{cc} = f'_{co} + f'_{cs}$. Table 1 shows the summary of the steel-based confinement models. Except for the confinement model by Mander *et al.* (1998a), which adopted a "five-parameter" multiaxial failure surface, existing empirical models (e.g. Saaticioglu and Razvi 1992, Hoshikuma *et al.* 1997) expressed the increase in the compressive strength due to confining steel in terms of an effective confining pressure ($f'_{cs} = k_{l,s} p_s$) due to steel. The confined compressive strength of concrete with lateral steel reinforcement may be expressed as

$$f'_{cc} = f'_{co} + k_{l,s} p_s \tag{2}$$

where $p_s = \rho_s f_{ys}/2$ and $\rho_s = 4A_s/(ds)$. The confining pressure in Eq. (2) depends on the yield strength (f_{ys}) of the steel, core diameter (d), spacing of the transverse bar (s) and area of transverse bar (A_s). The models usually differ only on the assumed form of the confinement effectiveness coefficient ($k_{l,s}$) due to steel, which is usually derived from regression analysis of experimental data. Saaticioglu and Razvi (1992) expressed the coefficient in terms of the confining pressure (p_s) as an exponential function, which approaches a constant value in the high-pressure range. The model by Hoshikuma *et al.* (1997), which is adopted in the Japanese Road Association (JRA) Design Specification of Highway Bridges, derived a constant coefficient 3.83 for the peak stress based on their tests.

2.2 CFRP-confined concrete columns

Models specifically suited to FRP-confined concrete columns or cylinders have been proposed. Based on the review by De Lorenzis and Tepfers (2003), the three most accurate models are those by Samaan *et al.* (1998), Saafi *et al.* (1999) and Spoelstra and Monti (1999). Most of these models are empirical in nature and were calibrated to their own sets of experimental data. Li *et al.* (2003), on the other hand, adopted a confinement model (named the L-L model) based on the mechanism of soil under tri-axial loading and used the Mohr-Columb failure envelope for soil. Table 2 shows models for FRP-confined concrete columns or cylinders.

The confined compressive strength of concrete with FRP can be expressed as the sum of the unconfined compressive strength (f'_{co}) and the increase in strength due to FRP confinement (f'_{cf}) as

Table 2 FRP-based confinement models

Reference	Model
Saadatmanesh *et al.* (1994)	$f'_{cc} = f'_{co}(2.254\sqrt{1+7.94p_{u,FRP}/f'_{co}} - 2p_{u,FRP}/f'_{co} - 1.254)$ where $p_{u,FRP} = 2f_{FRP}nt/D = \rho_{FRP}f_{FRP}/2$
Samaan *et al.* (1998)	$f'_{cc} = f'_{co} + 6.0(2f_{FRP}nt/D)^{0.7}$
Saafi *et al.* (1999)	$f'_{cc} = f'_{co} + 2.2(2f_{FRP}nt/D)^{0.84}$
Spoelstra and Monti (1999)	$f'_{cc} = 0.2f'_{c0} + 3.0(2f_{FRP}nt/D)^{0.5}$
Li *et al.* (2003)	$f'_{cc} = f'_{c0} + k_c(2f_{FRP}nt/D)\tan^2(45+\phi/2)$ where $\phi = 36^o + f'_{co}/35 \le 45^o$ and $k_c = 0.95$ for circular section

$f'_{cc} = f'_{co} + f'_{cf}$. The increase in the compressive strength due to FRP can be expressed as $f'_{cf} = k_{l,FRP}p_u$ and the resulting general expression for confined compressive strength of concrete with FRP becomes

$$f'_{cc} = f'_{co} + k_{l,FRP}p_{u,FRP} \tag{3}$$

where $P_{u,FRP} = \rho_{FRP}f_{FRP}/2$ and $\rho_{FRP} = 4nt/D$. The confining pressure in Eq. (3) depends on the tensile strength (f_{FRP}) of the FRP, thickness of the FRP (t), number of FRP layers (n) and the column diameter (D).

2.3 Steel and/or FRP-confined columns

Existing reinforced concrete columns when retrofitted by wrapping FRP sheets around the cylinder will be confined in the inner core by the lateral steel reinforcement and externally by the FRP sheets. Columns using both steel reinforcements and FRP sheets as confining devices are referred to as "hybrid columns". In Fig. 2, the total lateral pressure exerted by the concrete core due to dilation of the column will be resisted by the two confining materials. From equilibrium, the confining pressure in the concrete core (neglecting concrete between CFRP and steel ties) may be expressed as

$$p(dL) = 2f_{ys}(A_s) + 2f_{FRP}(tL) \tag{4}$$

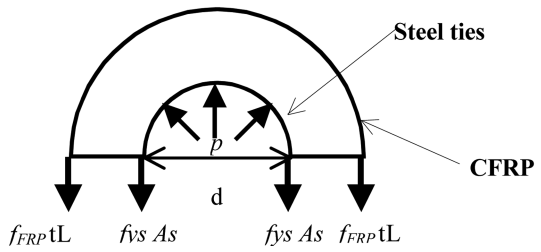

Fig. 2 Equilibrium of steel and CFRP-confined cylinder

Table 3 Confinement models for hybrid columns

Reference	Model
Hosotani and Kawashima (1999)	$f'_{cc} = f'_{co} + 2.2\rho_s f_{ys} + 1.93\rho_{FRP} f_{FRP}$
Li and Fang (2004)	$f'_{cc} = f'_{co} + (f'_1 + f'_2)\tan^2(45^\circ + \phi/2)$ $f'_1 = k_e \rho_s f_{ys}/2, f'_2 = k_c(2f_{FRP} nt/D)$ where $\phi = 36^\circ + f'_{co}/35 \le 45^\circ$, $k_e = (1 - s/2d)^n/(1 - \rho_{cc})$, n=1 for circular spirals and n=2 for circular hoops, and $k_c = 0.95$

The total lateral pressure may be multiplied by an effective confinement coefficient, k_l, to produce the effective total lateral pressure. The confined compressive strength of the concrete column may be expressed similar to Eq. (1) as $f'_{cc} = f'_{co} + k_l p$. It can be observed that the resulting confining pressure (p) in Eq. (4) is the due to the combined effects of the steel reinforcement and the FRP.

Table 3 presents two confinement models proposed for hybrid columns. In these models, the ultimate compressive strength, f'_{cc}, due to both confining materials is expressed as a superposition of the individual effects of steel ties and CFRP given as

$$f'_{cc} = f'_{co} + f'_{cs} + f'_{cf} \tag{5}$$

$$f'_{cc} = f'_{co} + k_{l,s} p_s + k_{l,FRP} p_{u,FRP} \tag{6}$$

The effective confining pressure due to each material device is derived separately and the contributions of each material are added as given by Eq. (6). Hosotani and Kawashima (1999) proposed an equation applicable to concrete confined by steel reinforcement, CFRP, and both steel reinforcement and CFRP. Regression analysis was used to derive the various coefficients in the equation using new experimental data. The steel-based model by Hoshikuma *et al.* (1997) was modified by adjusting the coefficient to extend the application to hybrid columns. Li and Fang (2004), on the other hand, modified the original L-L model (Li *et al.* 2003) to extend the application to concrete confined by steel reinforcement, CFRP, and both steel reinforcement and CFRP. In the proposed model, the lateral confining pressure due to steel reinforcement is based on the model by Mander *et al.* (1998a), while the lateral confining pressure contributed by the CFRP was based on the Mohr-Columb failure envelope of the L-L model.

3. Experimental data

Experimental data on confined concrete circular columns from various studies were compiled. The experimental data were classified into three groups based on the focus of the experiments. The first set of data (Steel Confined or SC data) in Table 4 represents the experiments focused on RC columns confined by lateral steel ties only. The lateral steel ties include spirals and hoops. The second set of data (CFRP Confined or CC data) in Table 5 represents the tests on columns or cylinders wrapped with CFRP only. No steel reinforcements – both longitudinal and lateral – were installed in the specimens. Finally, the third set of data (Steel and CFRP Confined or SCC data) in

Table 4 SC experimental data

Specimen	D (mm)	d (mm)	L (mm)	ρ_s (%)	ρ_{cc} (%)	f_{ys} (MPa)	ϕ (mm)	s (mm)	f'_c (MPa)	f'_{co} (Mpa)	Expt f'_{cc} (MPa)	ANN f'_{cc} (MPa)
Mander *et al.* (1998a)												
M-a	500	438	1500	2	1.6	310	12	52	28	24	38.00	42.19
M-b	500	438	1500	2	1.6	340	12	52	31	30	48.00	46.65
M-c	500	438	1500	2	1.6	340	12	52	33	32	47.00	47.11
M-1a	500	438	1500	2.5	1.6	340	12	41	28	29	51.00	50.62
M-2	500	438	1500	1.5	1.6	340	12	69	28	29	46.00	41.56
M-3a	500	438	1500	1	1.6	340	12	103	28	29	40.00	39.84
M-4	500	438	1500	0.6	1.59	320	10	119	28	29	36.00	36.02
M-5	500	438	1500	2	1.59	320	10	36	28	29	47.00	43.03
M-6	500	438	1500	2	1.63	307	160	93	28	29	46.00	42.15
M-7	500	438	1500	2	3.27	340	12	52	31	32	52.00	51.55
M-8	500	438	1500	2	3.3	340	12	52	27	30	49.00	49.29
M-9a	500	438	1500	2	2.34	340	12	52	31	32	52.00	52.10
M-10	500	438	1500	2	3.2	340	12	52	27	30	50.00	49.36
M-11	500	438	1500	2	4.8	340	12	52	27	30	54.00	53.87
M-12	500	438	1500	2	3.2	340	12	52	31	32	52.00	51.82
Sakai (2000)												
N-1	200	185	600	0.57	1.18	376	6.35	120	29.8	24.6	29.60	31.25
N-2a	200	185	600	1.14	1.18	376	6.35	60	29.8	24.6	29.70	33.59
N-2b	200	185	600	1.14	1.18	376	6.35	60	29.8	24.6	34.40	33.59
N-3	200	185	600	1.71	1.18	376	6.35	40	29.8	24.6	35.90	36.76
D-1a	200	185	600	0.57	1.18	376	2 × 6.35	240	29.8	24.6	31.10	31.25
D-2	200	185	600	1.14	1.18	376	2 × 6.35	120	29.8	24.6	36.00	33.59
D-3	200	185	600	1.71	1.18	376	2 × 6.35	80	29.8	24.6	36.10	36.76
Sakai(2001)												
C1-20	300	280	900	2.26	1.85	363	6.35	20	19.45	21	35.40	34.81
C1-30	300	280	900	1.51	1.85	363	6.35	30	19.45	21	29.70	26.65
C1-40	300	280	900	1.31	1.85	363	6.35	40	19.45	21	27.00	25.35
C1-60a	300	280	900	0.75	1.85	363	6.35	60	19.45	21	24.00	22.17
C1-80	300	280	900	0.57	1.85	363	6.35	80	19.45	21	22.80	21.19
C1-120	300	280	900	0.38	1.85	363	6.35	120	19.45	21	19.80	20.16
C1-160	300	280	900	0.28	1.85	363	6.35	160	19.45	21	19.30	19.62
C2-40	300	280	900	2.26	1.85	363	2×6.35	40	19.45	21	33.80	34.81
C2-60	300	280	900	1.51	1.85	363	2×6.35	60	19.45	21	27.80	26.65
C2-80a	300	280	900	1.31	1.85	363	2×6.35	80	19.45	21	25.40	25.35
C2-120	300	280	900	0.75	1.85	363	2×6.35	120	19.45	21	22.30	22.17
C2-160	300	280	900	0.57	1.85	363	2×6.35	160	19.45	21	20.10	21.19
C3-60	300	280	900	2.26	1.85	363	3×6.35	60	19.45	21	34.10	34.81
C3-80a	300	280	900	1.7	1.85	363	3×6.35	80	19.45	21	26.70	28.09
C3-120	300	280	900	1.13	1.85	363	3×6.35	120	19.45	21	22.40	24.28
C3-160a	300	280	900	0.85	1.85	363	3×6.35	160	19.45	21	20.30	22.71

Table 4 Continued

Hoshikuma (1997)

Specimen	D (mm)	d (mm)	L (mm)	ρ_s (%)	ρ_{cc} (%)	f_{ys} (MPa)	ϕ (mm)	s (mm)	f'_c (MPa)	f'_{co} (Mpa)	Expt f'_{cc} (MPa)	ANN f'_{cc} (MPa)
SC0	200	0	600	0	0	0	6	0	NA	18.5	18.53	18.60
SC1	200	200	600	0.39	0	235	6	150	NA	18.5	22.16	21.87
SC2	200	200	600	0.58	0	235	6	100	NA	18.5	24.42	24.67
SC3	200	200	600	1.17	0	235	6	50	NA	18.5	30.50	30.89
SC4	200	200	600	2.33	0	235	6	25	NA	18.5	38.00	37.95
SC5	200	200	600	4.66	0	235	6	12.5	NA	18.5	59.92	59.98
LC0	500	500	1500	0	1.01	295	0	0	NA	28.8	28.83	30.14
LC1	500	500	1500	0.19	1.01	295	10	300	NA	28.8	32.26	31.94
LC2	500	500	1500	0.39	1.01	295	10	150	NA	28.8	40.80	34.15
LC3	500	500	1500	0.58	1.01	295	10	100	NA	28.8	37.17	36.55
LC4	500	500	1500	1.16	1.01	295	10	50	NA	28.8	43.93	44.39
LC5	500	500	1500	0.34	1.01	295	13	300	NA	28.8	33.05	33.57
LC6	500	500	1500	0.54	1.01	295	16	300	NA	28.8	37.36	36.03

Table 5 CC experimental data

Karabinis and Rousakis(2002)

Specimen	D (mm)	L (mm)	ρ_{FRP} (%)	t (mm)	n layer	f'_c (MPa)	f'_{co} (MPa)	E (GPa)	f_{FRP} (MPa)	Expt f'_{cc} (MPa)	ANN f'_{cc} (MPa)
C1-3	200	320	0.234	0.117	1	NA	38.5	240	3720	43.53	42.91
C4-6	200	320	0.234	0.117	1	NA	35.7	240	3720	41.83	42.25
C7-9	200	320	0.468	0.117	2	NA	38.5	240	3720	52.17	50.26
C10-12	200	320	0.468	0.117	2	NA	35.7	240	3720	49.50	51.21
C13-15	200	320	0.702	0.117	3	NA	38.5	240	3720	54.50	58.42
C16-18	200	320	0.702	0.117	3	NA	35.7	240	3720	65.33	60.47
Miyauchi *et al.* (1997)											
MI1	150	300	0.29	0.11	1	45.20	45.20	230.5	3481	59.40	59.31
MI2	150	300	0.59	0.11	2	45.20	45.20	230.5	3481	79.40	70.13
MI3	150	300	0.29	0.11	1	31.20	31.20	230.5	3481	52.40	54.05
MI4	150	300	0.59	0.11	2	31.20	31.20	230.5	3481	67.40	68.07
MI5	150	300	0.88	0.11	3	31.20	31.20	230.5	3481	81.70	81.32
Rousakis (2001)											
RO1-3	150	300	0.45	0.169	1	25.15	25.15	118.34	2024	41.48	41.12
RO4-6	150	300	0.90	0.169	2	25.15	25.15	118.34	2024	59.21	55.09
RO7-9	150	300	1.35	0.169	3	25.15	25.15	118.34	2024	68.15	68.26
RO10-12	150	300	0.45	0.169	1	47.44	47.44	118.34	2024	67.62	67.26
RO13-15	150	300	0.90	0.169	2	47.44	47.44	118.34	2024	81.27	83.63
RO16-18	150	300	1.35	0.169	3	47.44	47.44	118.34	2024	98.49	97.78
RO19-21	150	300	0.45	0.169	1	51.84	51.84	118.34	2024	76.86	73.3

Table 5 Continued

Specimen	D (mm)	L (mm)	ρ_{FRP} (%)	t (mm)	n layer	f'_c (MPa)	f'_{co} (MPa)	E (GPa)	f_{FRP} (MPa)	Expt f'_{cc} (MPa)	ANN f'_{cc} (MPa)
RO22-24	150	300	0.90	0.169	2	51.84	51.84	118.34	2024	92.12	90.34
RO25-27	150	300	1.35	0.169	3	51.84	51.84	118.34	2024	110.46	107.13
RO28-30	150	300	2.25	0.169	5	51.84	51.84	118.34	2024	125.76	125.81
R031-033	150	300	0.45	0.169	1	70.48	70.48	118.34	2024	84.85	85.26
RO34-36	150	300	0.90	0.169	2	70.48	70.48	118.34	2024	99.80	99.55
RO37-39	150	300	1.35	0.169	3	70.48	70.48	118.34	2024	110.86	120.43
RO40-42	150	300	0.45	0.169	1	82.13	82.13	118.34	2024	95.84	95.71
RO43-45	150	300	0.90	0.169	2	82.13	82.13	118.34	2024	98.17	107.73
RO48	150	300	1.35	0.169	3	82.13	82.13	118.34	2024	124.71	124.64

Table 6 presents experiments on columns confined with steel ties and/or CFRP. These three sets of data were divided into two sets – training and testing data. The highlighted data in the tables represents the testing data.

3.1 Steel confined data

Table 4 shows the experiments conducted by Mander *et al.* (1998b) on 15 columns with 500 mm diameter and 1,500 mm height. The core diameters of the columns are 438 mm. All columns consist of spirals as lateral reinforcements and longitudinal bars with varying sizes and spacing. In Table 4 are also shown, details of the experiments conducted by Sakai *et al.* (2000). The circular columns have 200 mm diameter and 600 mm height. The columns were provided with both lateral ties and longitudinal bars (10 bars with 6.35 mm diameter). The N series are those provided with only one layer of lateral reinforcement, while the D series consists of two layers of lateral reinforcements. Another set of experiments were conducted by Sakai (2001). The 16 columns are of 300 mm diameter (280 mm core diameter) and 900 mm in height. Sixteen longitudinal bars with diameter of 9.53 mm were provided. C1, C2 and C3 correspond to one, two and three layers of lateral reinforcement with 6.35 mm diameter, respectively. Two sets of circular columns were tested by Hoshikuma *et al.* (1997). The SC columns are 200 mm diameter and 600 mm in height with no longitudinal steel, while the LC columns are 500 mm diameter and 1500 mm in height with longitudinal steel. No concrete cover was provided in all columns, meaning the column diameter is also the core diameter. There was no information provided for the unconfined cylinder strength of concrete, f'_c.

3.2 CFRP confined data

In Table 5, Karabinis and Rousakis (2002) conducted tests on cylindrical specimens 200×320 mm (height to diameter ratio 1:6) confined by CFRP sheets under axial load. The specimens were wrapped with relatively low confinement volumetric ratios (0.23-0.70%) so as to examine their confining effect when FRP sheets are used as reinforcement in rehabilitation. Two types of concrete mixtures were used with strength 47.5 and 43.5 MPa. All specimens were wrapped with CFRP having an overlap of 160 mm in the external layer. Note that three specimens are used for the same

Table 6 SCC experimental data

Specimen	D (mm)	d (mm)	L (mm)	ρ_s (%)	ρ_{cc} (%)	f_{ys} (MPa)	ϕ (mm)	s (mm)	ρ_{FRP} (%)	t (mm)	n layer	f'_c (MPa)	f'_{co} (MPa)	EFRP (GPa)	f_{FRP} (MPa)	Expt f'_{cc} (MPa)	ANN f'_{cc} (MPa)
Hosotani and Kawashima (1999)																	
C-1a	200	185	600	0	0.95	235	6	0	0	0	0	NA	38.51	0	0	38.52	37.54
C-1b	200	185	600	0	0.95	235	6	0	0	0	0	NA	42.92	0	0	42.94	43.11
C-1c	200	185	600	0	0.95	235	6	0	0	0	0	NA	44.8	0	0	44.81	44.89
C-2	200	185	600	0.41	0.95	235	6	150	0	0	0	NA	38.51	0	0	39.67	39.17
C-3	200	185	600	0.62	0.95	235	6	100	0	0	0	NA	38.51	0	0	39.38	41.16
C-4	200	185	600	1.24	0.95	235	6	50	0	0	0	NA	38.51	0	0	54.58	53.53
C-5	200	185	600	0	0.95	235	6	0	0.056	0.111	0.25	NA	38.51	243	4227	38.42	37.09
C-6	200	185	600	0.41	0.95	235	6	150	0.056	0.111	0.25	NA	38.51	243	4119	38.52	40.03
C-7	200	185	600	0.62	0.95	235	6	100	0.056	0.111	0.25	NA	38.51	243	4119	42.69	42.04
C-8	200	185	600	1.24	0.95	235	6	50	0.056	0.111	0.25	NA	38.51	243	4119	49.84	49.35
C-9	200	185	600	0	0.95	235	6	0	0.111	0.111	0.5	NA	38.51	243	4227	38.94	38.87
C-10	200	185	600	0.41	0.95	235	6	150	0.111	0.111	0.5	NA	38.51	243	4227	40.58	41.49
C-11	200	185	600	0.62	0.95	235	6	100	0.111	0.111	0.5	NA	38.51	243	4227	41.66	43.71
C-12	200	185	600	1.24	0.95	235	6	50	0.111	0.111	0.5	NA	38.51	243	4227	46.30	50.82
C-13	200	185	600	0	0.95	235	6	0	0.167	0.111	0.75	NA	38.51	243	4227	40.07	40.8
C-14	200	185	600	0.41	0.95	235	6	150	0.167	0.111	0.75	NA	38.51	235	4403	45.32	42.67
C-15	200	185	600	0.62	0.95	235	6	100	0.167	0.111	0.75	NA	44.8	235	4403	47.95	47.42
C-16	200	185	600	1.24	0.95	235	6	50	0.167	0.111	0.75	NA	38.51	243	4119	52.43	53.77
C-17	200	185	600	0	0.95	235	6	0	1.336	0.167	4	NA	42.92	252	4433	91.94	92.23
C-18	200	185	600	0.41	0.95	235	6	150	1.336	0.167	4	NA	38.51	249	4178	96.77	96.71
C-19	200	185	600	0.62	0.95	235	6	100	1.336	0.167	4	NA	38.51	249	4178	96.54	96.79
C-20	200	185	600	1.24	0.95	235	6	50	1.336	0.167	4	NA	38.51	249	4178	96.48	96.59
Li and Fang (2004)																	
A-0	300	250	600	1.14	0.76	274.7	9.52	100	0	0.11	0	17.2	16.68	230.535	0	17.96	18.8
A-1	300	250	600	1.14	0.76	274.7	9.52	100	0.1467	0.11	1	17.2	16.68	230.535	4120.2	32.27	32.48
A-2	300	250	600	1.14	0.76	274.7	9.52	100	0.2933	0.11	2	17.2	16.68	230.535	4120.2	39.89	39.99
B-0	300	250	600	1.14	0.76	274.7	9.52	100	0	0.11	0	17.2	16.68	230.535	0	18.42	18.8
B-1	300	250	600	1.14	0.76	274.7	9.52	100	0.1467	0.11	1	17.2	16.68	230.535	4120.2	31.85	32.48
B-2	300	250	600	1.14	0.76	274.7	9.52	100	0.2933	0.11	2	17.2	16.68	230.535	4120.2	40.90	39.99
C-0	300	250	600	1.14	0.76	274.7	9.52	100	0	0.11	0	17.2	16.68	230.535	0	20.05	18.8
C-1	300	250	600	1.14	0.76	274.7	9.52	100	0.1467	0.11	1	17.2	16.68	230.535	4120.2	33.13	32.48
C-2	300	250	600	1.14	0.76	274.7	9.52	100	0.2933	0.11	2	17.2	16.68	230.535	4120.2	39.87	39.99
D-0	300	0	600	0	0	0	9.52	100	0	0.11	0	17.2	16.68	230.535	0	16.68	16.65
D-1	300	0	600	0	0	0	9.52	100	0.1467	0.11	1	17.2	16.68	230.535	4120.2	25.52	25.47

material and section properties (e.g. C1, C2 and C3 represent the same column). Hence, the average values of the confined compressive strength (f'_{cc}) for each three specimens are used in the modeling resulting to six sets of data only. In the experiments by Miyauchi *et al.* (1997) the 150×300 mm cylinders confined with CFRP only, have overlaps of 60 mm in the outer cylinder and 40 mm on the inner part. CFRP sheets with 0.11 mm thickness were wrapped in one, two and three layers. Rousakis (2001) used CFRP sheets with 0.16 mm thickness that were wrapped at one, two and three layers around 150×300 mm cylinders with overlaps of 150-160 mm. Three specimens for a column with the same material and section properties (e.g. R01, R02 and R03 represent the same column) were used. Hence, the average values of the confined compressive strength (f'_{cc}) for columns with similar properties are used in the modeling.

3.3 Steel and CFRP confined data

In Table 6, cylinders with 200 mm in diameter and 600 mm in height were subjected to axial loading by Hosotani and Kawashima (1999). The cylinders were wrapped with CFRP with volumetric ratio ranging from 0.056% to 1.336%. The overlap length was 100 mm at the ends. Sliced 10-30 mm wide CFRP sheets was used for cylinders with CFRP volumetric ratio ≤ 0.167%, since the ratio will be too high if a whole CFRP is wrapped. Two types of CFRP were used depending on the amount of carbon fiber (200 g/m^2 or 300 g/m^2) – each corresponding to different thickness (0.110 mm or ≤ 0.167 mm, respectively). In this table a theoretical value for the number of layers was estimated for specimens with CFRP volumetric ratio ≤ 0.167%, given the thickness of CFRP sheet.

Li and Fang (2004) conducted tests on 36 concrete cylinders divided into four groups and each group having nil, one and two layers of CFRP with an overlap of about 100 mm. The four groups of tests correspond to different types of steel reinforcement such as circular hoop (A), two C-shaped lap-splice (B), circular spiral (C) and no steel reinforcement (D). For each group, three cylinders were tested and the average results are presented. The steel reinforcement used is No. 3 (9.52 mm diameter) and the yield strength is 274.7 MPa. The designed concrete strength is 17.2 MPa with a slump of 12 cm. There was no information about the longitudinal reinforcement, however, based on computations, an estimate of the amount of longitudinal steel of about 0.76 % corresponding to six bars with diameter of 10 mm is obtained.

4. Neural network-based confinement model

4.1 Neural network concepts

An artificial neural network (ANN) is a collection of simple processing units or neurons connected through links called connections. The topology or architecture of a three-layer feedforward neural network may be presented schematically, as in Fig. 3. The neural network is represented in the form of a directed graph, where the nodes represent the neuron or processing unit, the arcs represent the connections with the normal direction of signal flow is from left to right. The processing units may be grouped into layers of input, hidden and output neurons. The neural network in the figure consists of two input neurons, two hidden neurons and one output neuron. The main tasks of neurons are to receive input from its neighboring units, which provide incoming activations,

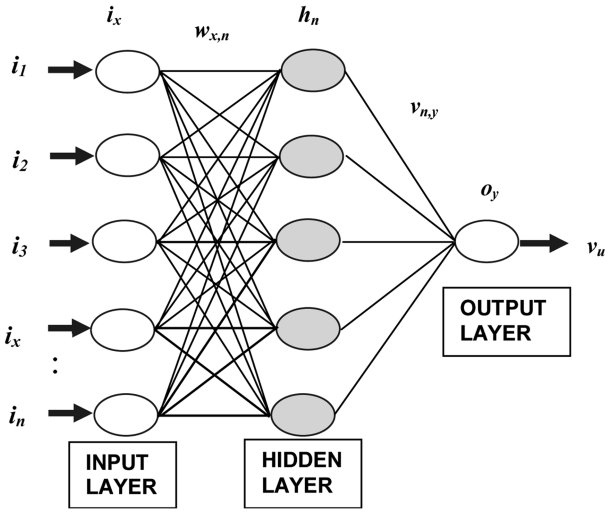

Fig. 3 A multi-layered feed-forward neural network

compute an output by using an activation function, and send that output to its neighbors receiving its output. The strength of the connections among the processing units is provided by a set of weights that affect the magnitude of the input that will be received by the neighboring units. The values of the connection weights are determined by training a neural network.

The following equations describe the mode of operation of a three-layer feedforward network in Fig. 3

$$\boldsymbol{h_n} = \boldsymbol{f}\left(\sum_{\boldsymbol{x}=1}^{\boldsymbol{M}} (\boldsymbol{w_{x,n}} \cdot \boldsymbol{i}) + \boldsymbol{b_n}\right) \tag{7}$$

$$\boldsymbol{o_y} = \boldsymbol{f}\left(\sum_{\boldsymbol{n}=1}^{\boldsymbol{N}} (\boldsymbol{v_{n,y}} \cdot \boldsymbol{h_n}) + \boldsymbol{b_y}\right) \tag{8}$$

Where i_x = scaled input value transmitted from the xth input neuron; h_n = activity level generated at the nth hidden neuron; o_y= activity level generated at the yth output neuron; $w_{x,n}$ and $v_{n,y}$ = weights on the connections to the hidden and output layers of neurons, respectively; b_n and b_y = weighted biases and f [ ] = activation or transfer function.

The training phase of an ANN is implemented by using a learning algorithm such as Levenberg-Marquardt algorithm. The main objective in the training phase is to find a set of weights, which produces minimum error. The learning algorithm is implemented in the training phase of the neural network implementation. In the training phase, a set of training data are used as inputs and outputs. Usually, an error criterion for the network output is chosen and the maximum number of cycles is set to provide a condition for terminating the simulations. The performance of the ANNs can be monitored by taking note of the convergence behavior of the error with respect to the number of cycles. It can be observed that if the network "learns", the error will approach a minimum value. After the training phase, the ANNs can be tested for other input data. No weight modification is involved in the testing phase.

An ANN model, after it has been trained by presenting it with a set of training patterns, has to be empirically validated. The usual practice for ANN model validation is to evaluate the network performance measure using a selected error metric based on data (referred to as test data) that was not used in the training. Aside from validating the trained network, this performance measure is often used in research to show the superiority of certain network architecture. The evaluation and validation of an ANN prediction model can be done by using common error metrics such as the mean absolute error (MAE) or root mean squared error (RMSE). Another test for the model is the Pearson product moment correlation coefficient, R. The R-value reflects the extent of the linear relationship between two data sets - for example the R value between the set of predicted values of a model and the set of experimental values. A value of R equal to 1.0 means that the predicted values are equal to the experimental values. – a perfect linear fit! Hence, a model with value of R very close to one represents a superior model, when the predicted and experimental values are compared.

4.2 Training and testing neural network models

There were a total of 111 experimental data for the combined SC, CC and SCC data sets. The data sets were randomly grouped as training and test data (76 training and 35 testing). The highlighted data in Tables 4, 5 and 6 represent the testing data. From the experimental database, there are fifteen column parameters that are available as shown in Table 7.

There are two values of unconfined compressive strength of concrete. One is given as the unconfined compressive strength (f'_c) of a cylinder (150 mm diameter by 300 mm height) and the other value is the unconfined compressive strength of the actual size (f'_{co}) of a column. In modeling, it is practical to use the value f'_c as a parameter instead of f'_{co} since it is easier and more economical to determine f'_c experimentally. It can be observed that the two values are very close; hence in the

Table 7 Summary of parameters from experimental data

No.	Symbol	Description
1	D	Column diameter
2	d	Core diameter
3	L	Column height
4	ρ_s	Ratio of volume of lateral reinforcement to volume of confined concrete core
5	A_s	Area of transverse bar
6	s	Spacing of the transverse bar
7	ρ_{cc}	Ratio of longitudinal steel to area of core of section
8	f_{ys}	Yield strength of lateral steel reinforcement
9	ρ_{FRP}	Ratio of volume of FRP to volume of concrete core
10	n	Number of layers wrapped around a cylinder
11	t	Thickness of the FRP sheet
12	f_{FRP}	Tensile strength of FRP sheet
13	f'_c	Compressive strength of unconfined concrete cylinder
14	f'_{co}	Compressive strength of unconfined concrete specimen of same size and geometry
15	f'_{cc}	Compressive strength or peak stress of confined concrete specimen

Table 8 Summary of experimental data

		Number of data	Geometric Properties of Specimens			Steel	CFRP		Concrete	
			D (mm)	d (mm)	L (mm)	f_{ys} (MPa)	t (mm)	f_{CFRP} (MPa)	f'_c (MPa)	f'_{co} (MPa)
SC set	Mander *et al.* (1998b)	15	500	438	1500	307-340			27-31	24-32
	Sakai *et al.* (2000)	7	200	185	600	376			29.8	24.6
	Sakai (2001)	16	300	280	900	363			19.45	21
	Hoshikuma (1997)	13	200 &500	200 &500	600 &1500	235 &295			NA	18.5 &28.8
CC set	Karabinis and Rousakis (2002)	6	200		320		0.117-0.351	3720	41-67.5	33.9-38.5
	Miyauchi *et al.* (1997)	5	150		300		0.11-0.33	3481	31.2-45.2	31.2-45.2
	Rousakis (2001)	16	150		300		0.169-0.845	2024	25.15-82.13	25.15-82.13
SCC set	Hosotani and Kawashima (1999)	22	200	185	600	235	0-2.67	4419-4403	NA	38.51-44.8
	Li and Fang (2004)	11	300	250	600	274.7	0.11-0.22	4120.2	17.2	16.68

Table 9 Parameters of ANN confinement models

Model	Input parameters	Output parameter
SCC9-x-1B	D, d, L, ρ_s, ρ_{cc}, ρ_{FRP} f_{ys}, f_{FRP}, f'_c	f'_{cc}
SCC10-x-1C	D, d, L, A_s, s, ρ_{cc}, nt, f_{ys}, f_{FRP}, f'_c	f'_{cc}

absence of the value of f'_{co}, it was assumed that $f'_c = f'_{co}$. A summary of the range of values from experimental data are shown in Table 8.

Based on the available parameters, two types of ANN models with different input parameters as shown in Table 9 were considered. The notation used in identifying the models are based on the neural network architecture (e.g. the model SCC9-x-1B means that it has nine input parameters, "x" number of hidden layer nodes, and one output parameter). The two models have similar input parameters (D, d, L, ρ_{cc}, f_{ys}, f_{FRP}, f'_c) except for the parameters related to the amount of confining steel and CFRP materials - SCC9-x-1B models used ρ_s, and ρ_{FRP}, while SCC10-x1C models used A_s, s, nt. The number of hidden layer nodes "x" was varied and the results of the simulations for training and testing are shown in the Table 10. Presented are the R-values and the maximum absolute error for both training and test data.

Comparing the results in Table 10 (a and b), the SCC9-x-1B models that use ρ_s, as a parameter for the amount of transverse steel reinforcement perform better especially in the testing phase yielding larger values for R ($\geq$ 0.98) and smaller maximum absolute error (less than 17 MPa) as compared with SCC10-x-1C where the best R = 0.9670 in the testing phase. Among the B models, the SCC9-7-1B had the best performance based on the R values and maximum absolute error especially during the testing phase. This model has the following error metrics for the testing phase: MAE of 2.4685 MPa, RMSE of 3.6257 MPa, R of 0.9891 and a maximum absolute error of 9.5691

Table 10 Training and testing results

(a) SCC9-x-1B

SCC9-x-1	SCC9-5-1	SCC9-6-1	SCC9-7-1	SCC9-8-1	SCC9-9-1	SCC9-10-1	SCC9-11-1
R training	0.9986	0.9986	0.9986	0.9986	0.9986	0.9986	0.9986
R testing	0.9852	0.9779	0.9891	0.9872	0.9820	0.9845	0.9855
Max.abs.error in training	4.7344	4.6167	4.8599	4.4160	4.4381	4.7506	4.5530
Max.abs.error in testing	13.0096	17.2633	9.5691	11.6493	15.4215	11.4310	16.9554

(b) SCC10-x-1C

SCC10-x-1	SCC10-5-1	SCC10-6-1	SCC10-7-1	SCC10-8-1	SCC10-9-1	SCC10-10-1	SCC10-11-1
R training	0.9959	0.9986	0.9986	0.9986	0.9987	0.9986	0.9986
R testing	0.9670	0.9459	0.9570	0.9601	0.9476	0.9077	0.9284
Max.abs.error in training	8.7082	5.7518	6.0169	4.1941	4.2145	4.4494	6.4380
Max.abs.error in testing	21.3181	23.6792	25.0744	29.1446	33.3512	39.5809	39.5093

Table 11 Connections weights of SCC9-7-1B ANN model

Input nodes to hidden layer nodes (Logsigmoid transfer function: $f(z) = 1/(1+e^{-z})$)

Hidden layer node	D	d	L	ρ_s	ρ_{cc}	ρ_{FRP}	f_{ys}	f_{FRP}	f'_c	*bias*
Node 1	0.6836	-15.1934	8.1087	-10.4127	11.1337	-1.8683	10.8999	-9.3006	2.2746	-2.0553
Node 2	-0.5152	2.8290	-1.9088	-2.6134	6.8687	-2.9533	13.1618	17.9628	16.2807	-16.4768
Node 3	8.6657	2.1792	1.4437	2.9076	5.6949	-4.0069	-3.2074	-6.3865	1.1807	-4.2284
Node 4	-3.8540	-1.1155	-0.0312	0.6278	7.4616	6.3251	-0.1578	-2.2851	-6.5172	1.5490
Node 5	-14.5065	7.3330	0.4080	-1.0180	1.1623	1.1217	-2.0989	-1.9962	2.1535	-1.5693
Node 6	-0.0833	-3.1298	5.5605	2.4713	-13.0619	5.9461	-2.9993	0.3609	11.4624	3.1311
Node 7	-9.8648	-1.7955	-6.5685	-18.8317	1.3480	-10.7807	10.5050	-1.3187	-23.6710	13.8325

Hidden layer nodes to output node (Purelin transfer function: $f(z) = z$)

Node 1	Node 2	Node 3	Node 4	Node 5	Node 6	Node 7	bias
-0.2864	0.3191	0.3047	0.4762	1.8617	0.3612	0.1107	-0.4188

MPa. Hence SCC97-1B model was selected in this study. The connection weights and biases of the model are shown in Table 11. The activation function are log-sigmoid and purelin transfer functions for the input-to-hidden-layer and hidden-layer-to-output nodes, respectively. A Visual Basic program was created implementing the three-layered feedforward neural network using the derived connection weights. The executable program can be accessed at the author's website (http://mysite.dlsu.edu.ph/faculty/oretaa).

4.2.1 Performance of the model

The performance of the SCC9-7-1B model which has nine inputs (D, d, L, ρ_s, ρ_{cc}, ρ_{FRP}, f_{ys}, f_{FRP}, f'_c) and one output (f'_{cc}) is compared with the empirical and analytical models used for columns confined by (a) steel reinforcements only, (b) CFRP only, or (c) both steel reinforcement and CFRP.

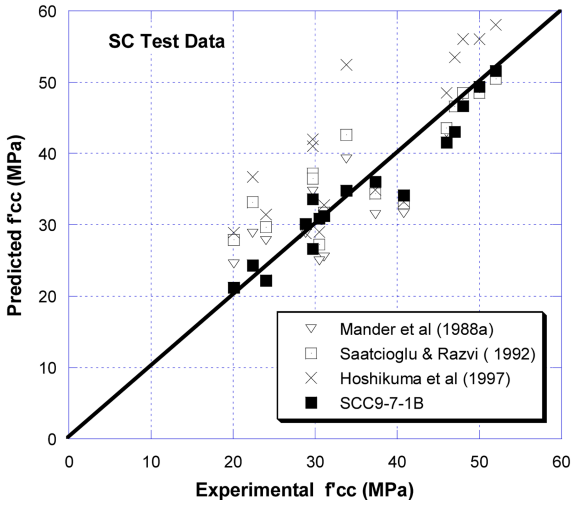

Fig. 4 Comparison of models for SC test data

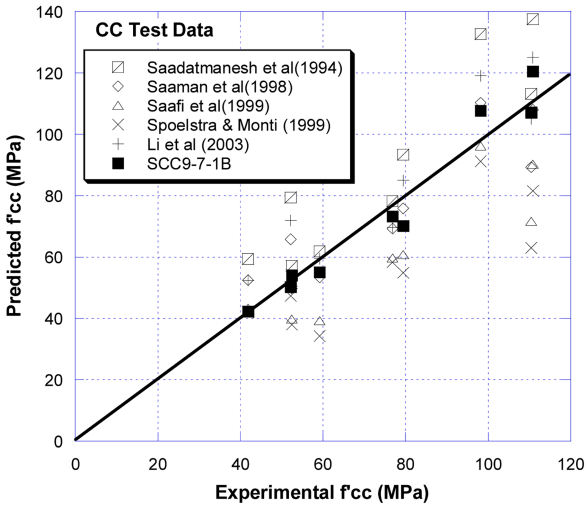

Fig. 5 Comparison of models for CC test data

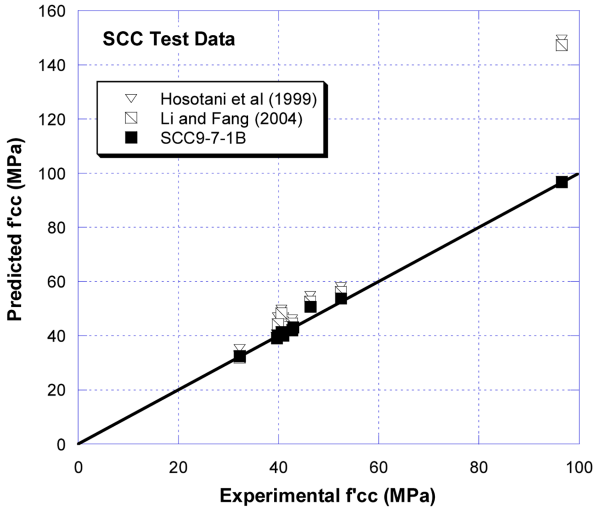

Fig. 6 Comparison of models for SCC test data

When the model is used for steel-confined columns only, the following parameters are set to zero: ρ_{FRP}, f_{FRP}, nt. On the other hand, if the model is used for CFRP-confined columns only with no longitudinal reinforcements, the following parameters are set to zero: d, ρ_s, ρ_{cc}, f_{ys}, A_s, s. The ANN model predictions for confined compressive strength for both training and test data are shown in the Tables 4, 5 and 6. The comparison of the model with the other empirical models are shown in Fig. 4, 5 and 6 for SC, CC and SCC test data, respectively. It can be observed from the figures that there is less scatter for the SCC9-7-1B model. Table 12 shows the comparison of the R-values of the different models when applied to the test data. The ANN model has R values of 0.9683, 0.9791 and 0.9964 for SC, CC and SCC Test data, respectively. The models of Hosotani and Kawashima (1999) and Li and Fang (2004) were also applied for SC, CC and SCC test data. The superior R-values of

Table 12 R-values of models using test data

Model	SC test data	CC test data	SCC test data
SCC9-7-1B	0.9683	0.9791	0.9964
Mander *et al.*	0.8878	-	-
Saatcioglu and Razvi (1992)	0.8606	-	-
Hoshikuma *et al.* (1997)	0.7992	-	-
Saadatmanesh *et al.* (1994)	-	0.9165	-
Samaan *et al.* (1998)	-	0.9032	-
Saafi *et al.* (1999)	-	0.8760	-
Spoelstra and Monti (1999)	-	0.8335	-
Li *et al.* (2003)	-	0.9274	-
Hosotani and Kawashima (1999)	0.8821	0.9287	0.9901
Li and Fang (2004)	0.9118	0.9274	0.9921

the ANN model when applied to columns confined with steel reinforcements only (SC), CFRP only (CC) and combined steel and CFRP (SCC) indicate that SCC9-7-1B model is a versatile model applicable not only to hybrid columns but also for steel or CFRP confined columns.

4.3.2 Application to retrofitting and strengthening

How can the ANN model for hybrid columns be used in practical applications? The present model can be used to estimate the increase in compressive strength of RC columns for strengthening or retrofitting using steel ties and/or CFRP. An existing reinforced concrete column confined with steel only can be retrofitted by using CFRP to increase its confined strength. Consider for example an RC column tested by Li and Fang (2004) confined with lateral ties only with the following

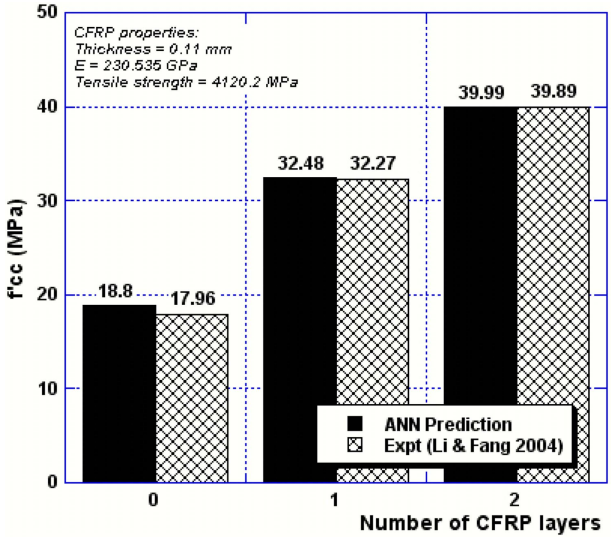

Fig. 7 Confined compressive strength of a column with varying CFRP layers

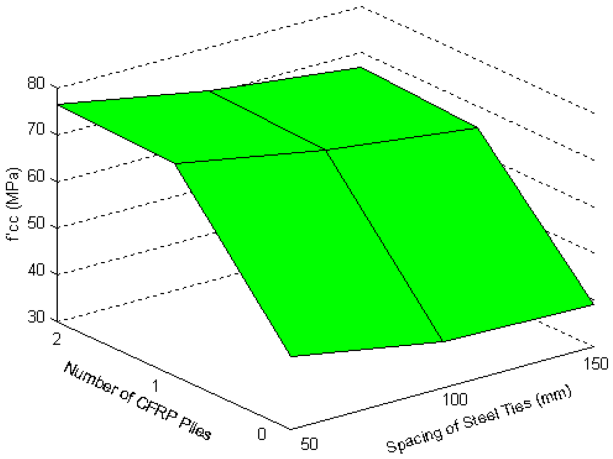

Fig. 8 Confined compressive strength of a column with varying steel spacing and CFRP layers

properties: D = 300 mm, d = 250 mm, L = 600 mm, ρ_s = 1.14%, ρ_{cc} = 0.76%, f_{ys} = 274.7 MPa, f'_c = 17.2 MPa and f'_{co} = 16.68 MPa. If the column will be strengthened by wrapping CFRP with thickness, t, of 0.11 mm and f_{FRP} = 4,120.2 MPa, how much strength will be gained? Fig. 7 shows the predicted confined compressive strength of the column with no CFRP (n = 0), one layer of CFRP (n = 1) and two layers of CFRP (n = 2) and the comparison with the experimental results. The predicted compressive strength of the column confined with steel only (n = 0) is 18.8 MPa compared to the experimental value of 17.96 MPa. When one layer of CFRP is wrapped, the predicted confined compressive strength increased to 32.48 MPa (about 73% increase with respect to n = 0). Wrapping two layers, increases the confined compressive strength to 39.99 MPa (more than 100% increase with respect to n = 0). The ANN predictions are relatively close to the experimental values. Through the predicted values of the confined compressive strength of the columns, a reasonable estimate of the capacity of existing RC structures can be done when retrofitted or strengthened with CFRP.

A parametric study where the amount of confining steel and CFRP are varied is shown in Fig. 8. The column has the following constant parameters similar to the specimens tested by by Mander *et al.* (1998b): D = 500 mm, d = 438 mm, L = 500 mm, ρ_{cc} = 1.6%, f_{ys} = 340MPa, lateral steel bar diameter = 12 mm, and f'_c = 28MPa. CFRP sheets with the properties of f_{FRP} = 3300 MPa, and thickness t = 0.11 mm are wrapped around this column. It can be seen that there is an abrupt increase of at least 65% in f'_{cc} from zero-ply to 1-ply of CFRP regardless of the spacing of lateral steel ties. Adding another ply of CFRP to a total of two plies yields an additional step size increase of about 1.8%.

5. Conclusions

The present study explored the use of new computational tools such as artificial neural networks (ANN) in predicting the confined compressive strength (f'_{cc}) of circular RC columns. By combining and re-analyzing existing experimental data on concrete columns confined by steel reinforcement and/or CFRP, a neural network model applicable to concrete columns confined by steel reinforcement

only, CFRP only, and both steel reinforcement and CFRP (hybrid columns) was developed. The present ANN model used as parameters for the confining materials the lateral steel ratio (ρ_s) and the FRP volumetric ratio (ρ_{FRP}). The SCC9-7-1B model gave good predictions for three types of confined columns: (a) columns confined with steel reinforcement only, (b) CFRP confined columns, and (c) hybrid columns confined by both steel and CFRP. The confinement of concrete by transverse steel reinforcement and/or CFRP improves the strength and ductility of reinforced concrete columns and bridge piers. Compressive strength enhancement due to confinement is reflected by an increase of the peak stress of the unconfined compressive strength (f'_{co}) to the confined compressive strength (f'_{cc}). The model can be used for predicting the compressive strength of existing circular RC columns confined with steel only that will be strengthened or retrofitted using CFRP.

Acknowledgements

This research was funded by the University Research Coordination Office (URCO) of De La Salle University-Manila, Philippines.

References

Cevik, A. and Guzelbey, I. (2008), "Neural network modeling of strength enhancement for CFRP confined concrete cylinders", *Build. Environ.*, **43**, 751-763.

Chuang, P.H., Goh, A.T.C. and Wu, X. (1998), "Modeling the capacity of pin-ended slender reinforced concrete columns using neural networks", *J. Struct. Eng. - ASCE*, **124**(7), 830-838.

De Lorenzis, L. and Tepfers, R. (2003), "A comparative study of models on confinement of concrete cylinders with fiber-reinforced polymers composites", *J. Compos. Constr. - ASCE*, **7**(3), 219-237.

Hoshikuma, J., Kawashima, K., Nagaya, K. and Taylor, A.W. (1997), "Stress-strain model for confined reinforced concrete in bridge piers", *J. Struct. Eng. - ASCE*, **123**(5), 624-633.

Hosotani, M. and Kawashima, K. (1999), "A stress-strain model for concrete cylinders confined by both carbon fiber sheets and tie reinforcement", *J. Concrete Eng. - JSCE*, **620**(43), 25-42. (in Japanese)

Karabinis, A.I. and Rousakis, T.C. (2002), "Concrete confined by FRP material: a plasticity approach", *Eng. Struct.*, **24**, 923-932.

Li, Y.F., Lin, C.T. and Sung, Y.Y. (2003), "A constitutive model for concrete confined with carbon fiber reinforced plastics", *Mech. Mater.*, **35**, 603-619.

Li, Y.F. and Fang, T.S. (2004), "A constitutive model for concrete confined by steel reinforcement and carbon fiber reinforced plastic sheet", *Struct. Eng. Mech.*, **18**(1), 21-40

Mander, J.B., Priestley, M.J.N. and Park, R. (1998a), "Theoretical stress-strain model for confined concrete", *J. Struct. Eng. - ASCE*, **114**(8), 1805-1826.

Mander, J.B., Priestley, M.J.N. and Park, R. (1998b), "Observed stress-strain behavior of confined concrete", *J. Struct. Eng. - ASCE*, **114**(8), 1827-1849.

Miyauchi, K., Nishibayashi, S. and Inoue, S. (1997), "Estimation of strengthening effects with carbon fiber sheet for concrete column", *Proc. FRPRCS-3*, Sapporo, Japan, Vol. 1, 217-224.

Oreta, A. and Kawashima, K. (2003), "Neural network modeling of confined compressive strength and strain of circular concrete columns", *J. Struct. Eng. - ASCE*, **129**(4), 554-561.

Rousakis, T. (2001), "Experimental investigation of concrete cylinders confined by carbon FRP sheets, under monotonic and cyclic axial compressive load", *Research Rep.*, Chalmers Univ. of Technology, Goteborg, Sweden.

Saadatmanesh, H., Ehsani, M.R. and Li, M.W. (1994), "Strength and ductility of concrete columns externally reinforced with fiber composite straps", *ACI Struct. J.*, **91**(4), 434-447.

Saafi, M., Toutanji, H. and Li, Zongjin (1999), "Behavior of concrete columns confined with fiber reinforced polymer tubes", *ACI Mater. J.*, **94**(4), 500-509.
Saatcioglu, M. and Razvi, S.R. (1992), "Strength and ductility of confined concrete", *J. Struct. Eng. - ASCE*, **118**(6), 1590-1607.
Sakai, J., Kawashima, K., Une, H. and Yoneda, K. (2000), "Effect of tie spacing on stress-strain relation of confined concrete", *J. Struct. Eng. - JSCE*, **46**(3), 757-766.
Sakai, J. (2001), "Effect of lateral confinement of concrete and varying axial load on seismic response of bridges", *Doctor of Engineering Dissertation*, Department of Civil Engineering, Tokyo Institute of Technology, Tokyo.
Samaan, M., Mirmiran, A. and Shahawy, M. (1998), "Model of concrete confined by fiber composites", *J. Struct. Eng. - ASC*E, **124**(9), 1025-1031.
Spoelstra, M.R. and Monti, G. (1999), "FRP-confined concrete model", *J. Compos. Constr.*, **3**(30), 143-150.

CC